Detection of Massive Tidal Tails around the Globular Cluster Pal 5 with SDSS Commissioning Data

Michael Odenkirchen[1], Eva K. Grebel[1], Constance M. Rockosi[2], Walter Dehnen[1], Rodrigo Ibata[1], Hans-Walter Rix[1], Andrea Stolte[1], Christian Wolf[1], John E. Anderson Jr.[3], Neta A. Bahcall[4], Jon Brinkmann[5], Istvan Csabai[6], G. Hennessy[7], Robert B. Hindsley[8], Željko Ivezić[4], Robert H. Lupton[4], Jeffrey A. Munn[9] Jeffrey R. Pier[9], Chris Stoughton[3], Donald G. York[2]

ABSTRACT

We report the discovery of two well-defined tidal tails emerging from the sparse remote globular cluster Palomar 5. These tails stretch out symmetrically to both sides of the cluster in the direction of constant Galactic latitude and subtend an angle of 2.6° on the sky. The tails have been detected in commissioning data of the Sloan Digital Sky Survey (SDSS), providing deep five-color photometry in a 2.5° wide band along the equator. The stars in the tails make up a substantial part ($\sim 1/3$) of the current total population of cluster stars in the magnitude interval $19.5 \leq i^* \leq 22.0$. This reveals that the cluster is subject to heavy mass loss. The orientation of the tails provides an important key for the determination of the cluster's Galactic orbit.

Subject headings: globular clusters: individual (Pal5) — Galaxy: halo — Galaxy: structure — Galaxy: kinematics and dynamics

1. Introduction

Globular clusters are self-gravitating stellar systems that experience a time-varying tidal potential as they orbit through their parent galaxy. Their dynamical evolution is driven by internal effects such as stellar evolution, two-body relaxation and binary heating, and by external effects induced by the galactic force field, i.e., heating by tidal shocks during disk and bulge passages and tidal stripping. Both internal and external effects should lead to a permanent loss of cluster members and to the eventual dissolution of the cluster. The Galactic globular clusters observed today are believed to be survivors from an initially much more numerous population. They appear to be in various stages of evolution and dissolution, depending on their initial conditions and their galactic orbits (e.g., Chernoff & Weinberg 1990, Djorgovsky & Meylan 1994). Numerical simulations predict that possibly as many as half of the present-day Galactic globulars will not survive for another Hubble time (Gnedin & Ostriker 1997). Observational confirmation of the gradual dissolution of globular clusters and determination of their mass loss rates is important in itself, but can also shed light on the formation history and structure of the Galactic halo and provide constraints on the Galactic potential.

[1]Max-Planck-Institut für Astronomie, Königstuhl 17, D-69117 Heidelberg, Germany; odenkirchen@mpia-hd.mpg.de, grebel@mpia-hd.mpg.de

[2]University of Chicago, Dept. of Astronomy & Astrophysics, 5640 South Ellis Ave., Chicago, IL 60637

[3]Fermi National Accelerator Laboratory, P.O. Box 500, Batavia, IL 60510

[4]Princeton University Observatory, Princeton, NJ 08544;

[5]Apache Point Observatory, P.O. Box 59, Sunspot, NM 88349-0059

[6]Dept. of Physics & Astronomy, The Johns Hopkins University, 3701 San Martin Drive, Baltimore, MD 21218

[7]U.S. Naval Observatory, 3450 Massachusetts Ave. NW, Washington, DC 20392-5420

[8]Naval Research Lab, 4555 Overlook Ave. SW, Washington, DC 20375

[9]U.S. Naval Observatory, Flagstaff Station, P.O. Box 1149, Flagstaff, AZ 86002-1149

TABLE 1
FUNDAMENTAL PARAMETERS OF PAL 5.

Parameter	Value	Reference
α, δ (J2000)	$229.02°, -0.11°$	
l, b	$0.9°, +45.9°$	
d	23.2 kpc	Harris (1996)
M	$1.3 \cdot 10^4 M_\odot$	Sandage & Hartwick (1977)
r_c	$2.9'$, 20 pc	Trager et al. (1995)
v_r	-56 km s^{-1}	Smith (1985)
$\mu_\alpha \cos\delta, \mu_\delta$	$(-2.44, -0.87)$ mas yr^{-1}	Schweitzer et al. (1993)
$\mu_\alpha \cos\delta, \mu_\delta$	$(-1.0, -2.7)$ mas yr^{-1}	Scholz et al. (1998)
$\mu_\alpha \cos\delta, \mu_\delta$	$(-2.55, -1.93)$ mas yr^{-1}	Cudworth (priv. comm.)

First signs of the existence of tidal debris around Galactic globular clusters were found in studies of globular cluster radial surface density profiles. In many cases the observed profiles deviate from the profile of a best-fit King model at the outermost radii and extend beyond the conventional limiting radius set by the model (e.g., Grillmair et al. 1995; Lehmann & Scholz 1997). Since the debris produced by a dissolving globular cluster will have similar orbital parameters as the cluster itself it is expected to drift away from the cluster in a leading and a trailing tail which are aligned with the cluster's orbit. Searches for such tidal tails in the vicinity of Galactic globular clusters require large area coverage and have so far been conducted with photographic material (Grillmair et al. 1995; Leon et al. 2000; Testa et al. 2000). While spatially distinct star count overdensities were detected around many clusters, density fluctuations caused by distant galaxy clusters, variable foreground reddening or photographic plate inhomogeneities have been found to be serious contaminants and have left the location and shape of the tidal tails in most cases uncertain.

The Sloan Digital Sky Survey (SDSS; see York et al. (2000); Gunn et al. (1998); Fukugita et al. (1996)) is designed to provide homogeneous, deep ($R \sim 23$) CCD imaging in five passbands (u', g', r', i', z') with contiguous coverage of $10^4 \square°$ in the Northern Galactic Cap. Such a high-quality database is ideally suited for studies of Galactic structure (e.g., Yanny et al. 2000; Ivezic et al. 2000) and lends itself in particular to searches for tidal debris with unprecedented depth and spatial coverage.

The SDSS commissioning scans happen to cover Palomar 5, a remote, sparse halo cluster. The peculiar characteristics of this cluster, i.e., very low mass, large core radius, and low central concentration (see Tab. 1) suggest that Pal 5 may have lost a significant amount of its initial mass and perhaps be close to disruption. Its radial velocity combined with determinations of its absolute proper motion suggest an eccentric orbit with passages through the Galactic disk inside the solar circle (Scholz et al. 1998).

In view of these indications we have searched the SDSS data for tidal debris around Pal 5. In Section 2 we describe our search method. Results are presented in Section 3.

2. Search method

In the current phase of SDSS, the region of Pal 5 is covered by an equatorial band with declinations $-1.25 \leq \delta \leq +1.25$. Our investigation concentrates on the range $226° \leq \alpha \leq 232°$, i.e., 3° east and west of the cluster, and on objects classified as SDSS point sources. The typical accuracy of the relative photometry in this data set is better than 0.03 mag for stars brighter than 20.0 mag in g^*, r^*, or i^*, and is ~ 0.1 mag at $u^* = 21.0, g^* = 22.2, r^* = 21.8, i^* = 21.4$, and $z^* = 20.0$ mag (* is used to indicate that the photometric zeropoints are still preliminary). In order to enable corrections for interstellar extinction the SDSS data provide individual extinction values based on the maps of Schlegel et al. (1998). These values (which are small in the field of Pal5)

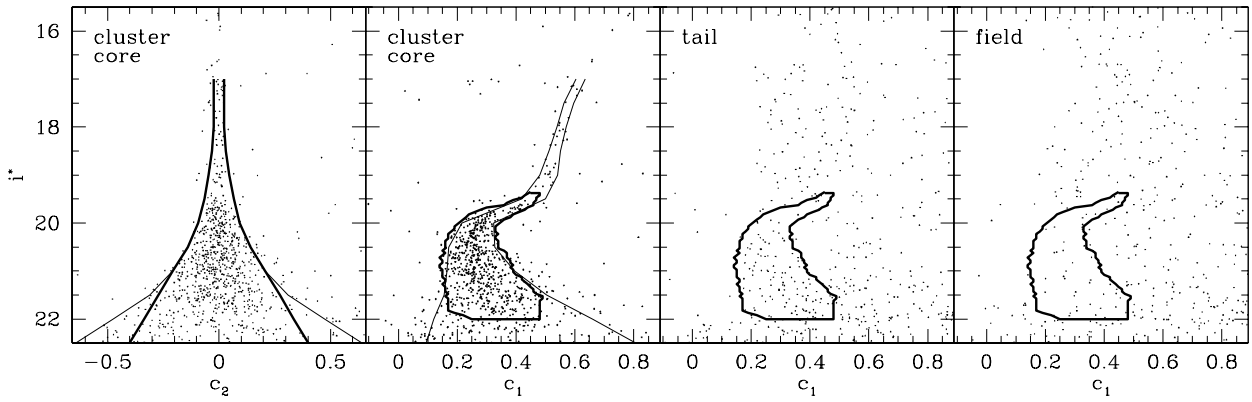

Fig. 1.— Color-magnitude diagrams for stellar SDSS sources in the field of Pal 5. From left to right: 1. (c_2, i^*) for objects within $3'$ of the cluster center (core). 2. (c_1, i^*) for objects within $3'$ of the cluster center (core). 3. (c_1, i^*) for objects in two circles centered on the cluster tails 4. (c_1, i^*) for objects in two circles in the outer field Note that the field sizes of the tail and field samples shown here are $8\times$ that of the core sample. The thick lines indicate our photometric selection criteria for cluster member candidates, the thin lines give 2σ-limits for the expected dispersion of cluster stars in c_1 and c_2 due to photometric errors.

have been subtracted from the observed stellar magnitudes.

One straightforward method for tracing the spatial distribution of cluster stars in a large field around a cluster is as follows: (i) Define the distribution of the cluster population in color-magnitude space by means of the stars near the cluster center, and that of the field stars by stars from a sufficiently distant part of the field. (ii) Determine the significance of each point in color-magnitude space by means of the local signal-to-noise ratio s of the expected true number of cluster stars, (i.e. the counted number of cluster stars minus the estimated number of contaminating field stars, see eq.(2)) in the surroundings of this point. (iii) Select those regions in color-magnitude space with high significance, i.e., with local signal-to-noise s above a certain threshold, extract from the entire sample all stars which lie in these particular color-magnitude regions, and analyze the spatial configuration of these stars.

This way of empirical photometric filtering was first described and used in the two-color study by Grillmair et al. (1995). It could, in principle, be easily generalized to a higher dimensional photometric space and thus be directly applied to the multimagnitude or multicolor-magnitude data of SDSS. However, in the case of the very sparse cluster Pal 5 it turned out that the number of cluster stars was too small to provide reasonable star count statistics in multidimensional color-magnitude cells. In order to avoid problems with noise from small numbers we thus worked with projections on color-magnitude planes, viz. those spanned by the magnitude i^* and the color indices $u^*-g^*, g^*-r^*, r^*-i^*$, and i^*-z^* or orthogonal combinations of the latter.

From g^*-r^* and r^*-i^* we tailored new color indices c_1, c_2 as given in eq. (1ab), with the advantage that for cluster stars the systematic variation of color with magnitude is mostly contained in c_1 while variations in c_2 are mostly random, i.e. due to natural spread and observational errors (see left panels of Fig.1).

$$c_1 = 0.907(g^*-r^*) + 0.421(r^*-i^*) \quad (1a)$$
$$c_2 = -0.421(g^*-r^*) + 0.907(r^*-i^*) \quad (1b)$$

The indices u^*-g^* and i^*-z^* were considered separately because they are less accurate than the others due to decreased sensitivity in the bluest and reddest photometric band.

As the first step of photometric filtering we applied simple magnitude-dependent color cuts in

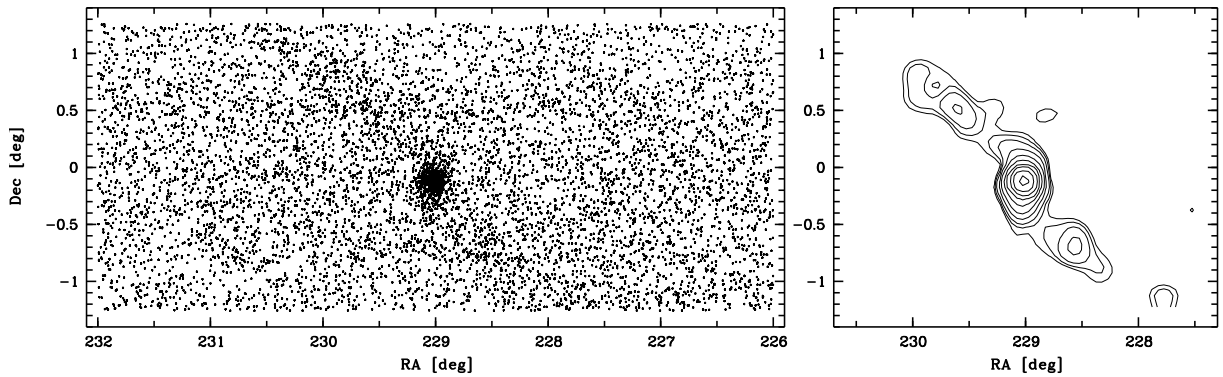

Fig. 2.— Projected spatial distribution of the photometric cluster member candidates selected with the method described in Section 2. Left: individual star positions. Right: contours of the surface density derived by adaptive kernel estimation. Contour levels are 0.19, 0.21, 0.24, 0.3, 0.4, 0.6, 1.0, 2.0, 4.0 and 8.0 stars/$\Box'$. The background has a mean of 0.13 stars/$\Box'$.

$u^* - g^*$, $i^* - z^*$, and c_2 according to the borders of the cluster population defined by stars from the cluster core ($r \leq 3'$), and according to the estimated spread due to photometric errors (for c_2 cf. leftmost panel of Fig. 1).

After this preselection, we used Grillmair's method for filtering in the color-magnitude plane of (c_1, i^*). The local signal-to-noise s of the expected true number of clusters stars was determined on a grid of mesh size 0.01 mag in c_1 and 0.05 mag in i^*. For each grid point (index k) the number $n_c(k)$ of stars in a circle of radius $12'$ around the cluster center and the number $n_f(k)$ of stars at more than 2° angular distance from the cluster center were counted in a color-magnitude box of width 0.09 mag in c_1 and 0.35 mag in i^* centered on that point. With n_c representing the number of cluster stars plus underlying field stars, n_f the number of field stars, and q the ratio of the areas on which n_f and n_c have been sampled, s was calculated as given by eq.(2).

$$s(k) = \frac{n_c(k) - q^{-1} n_f(k)}{\sqrt{n_c(k) + q^{-2} n_f(k)}} \qquad (2)$$

The size of the color-magnitude boxes and the overlap between boxes around neighboring grid points assure that s is a sufficiently smooth function. From the local signal-to-noise s one obtains a filtering mask in the (c_1, i^*) plane by setting a threshold $s_{lim} < s_{max}$ and by isolating the region in the grid (around the maximum of s) with $s \geq s_{lim}$. In order to find the most appropriate mask, we went through a series of gradually decreasing thresholds, counted for each threshold the cumulative number of stars in the corresponding mask in the area of the cluster's tails (N_t) and in the outer field (N_f), and determined from these numbers the cumulative signal-to-noise ratio SNR of the expected true number of cluster stars in the area of the tails (eq.(3)).

$$\mathrm{SNR} = \frac{N_t - w^{-1} N_f}{\sqrt{N_t + w^{-2} N_f}} \qquad (3)$$

The filtering mask was then chosen such that the cumulative signal-to noise reaches a maximum. As shown in Fig. 1 (second panel from left) this mask cuts out the zone from the bottom of the subgiant branch to the main-sequence turnoff and further down the main sequence to $i^* = 22.0$ mag. In the range $19.5 \leq i^* \leq 21.5$ the width of the mask approximately coincides with the 2σ limits for the dispersion of cluster stars in c_1 as derived from the median values of the estimated photometric errors. The two panels on the right in Fig. 1 give an example of the detection of cluster member candidates outside the cluster using the filter mask in the area of the cluster's tails and in the area of the outer field.

The spatial configuration of the complete sample of member candidates obtained by the photometric filtering process is shown in Fig. 2 (left panel). In the final step of data processing, the distribution of individual star positions was transformed into a smooth surface density function by means of adaptive kernel estimation (Silverman 1986). A standard parabolic kernel was used, with the kernel radius set to the angular distance of the 70th nearest neighbor of each star. This yields the surface density distribution shown in the contour plot of Fig. 2 (right panel).

3. Discussion

3.1. Characteristics of the tails

Fig. 2 shows that the density enhancements of point sources around the cluster form two spectacular tails which emerge from the cluster in northern and southern direction and turn over to the north-east and south-west, respectively, at angular distances of $\sim 0.2^\circ$ (80 pc in projected linear distance) from the cluster center. The tails stretch out almost symmetrically to both sides and exhibit clumps at a distance of $\sim 0.8^\circ$, i.e., 320 pc from the cluster. In total, the tails are visible along an arc of 2.6°. A weaker clump at the southern edge of the current field suggest that the tails might in fact continue to even larger distances.

In the two big clumps, the surface density of stars that fall inside our colour magnitude filter is about 2.3 times as high as in the surrounding field. Summing up the number of stars above background in the region of the tails and comparing them to the stars within a circle of radius $r < 12'$ around the cluster center we find that within our color-magnitude window the tails contain ~ 0.48 times the number of stars in the cluster. In other words, the tails comprise $\sim 32\%$ of the currently detected total population of cluster stars at and below the main-sequence turnoff. This is a rough (but conservative) estimate because the object is seen in a non-face-on projection which does not reveal a clear border between cluster and tail. Nonetheless it gives impressive evidence for heavy mass loss, confirming conjectures drawn from the low mass and low concentration of the cluster.

The structure of the observed tails follows the principal expectations for tidal tails and closely agrees with the results of recent N-body simulations of globular cluster tides (Combes et al. 2000). Basically, cluster members drift to the outer part of the cluster after acceleration in disk or bulge shocks and leave the cluster in the vicinity of the (Lagrange-) points of force balance between the cluster and the tidal field, i.e., in the direction to the galactic center and anticenter. Due to differential galactic rotation their trajectories then bend around and continue approximately parallel to the orbit of the cluster. The appearance of clumps in the tails is also supported by numerical simulations. They can either be caused by the enhanced release of particles after strong shock events or by caustics of the trajectories in phase space.

3.2. The role of contaminants

In view of the striking resemblance of the detected structures to the expected properties of tidal tails, significant contamination by clustered background objects seems a priori unlikely. Nevertheless we checked this point by analysing the density and colors of non-pointlike SDSS sources around Pal 5 which by their shape are classified as galaxies. Their spatial distribution is clumped and reveals known galaxy clusters like Abell 2050 and 2035. However, most of these sources do not fall into the color-magnitude window for members of Pal 5. If our selection criteria for Pal 5 members are applied to the galaxy sample, the surface density of galaxies drops to the level of 0.3 to 0.6 of the field background density of the stellar sample. Moreover, the pattern of density variations in the galaxy sample does not correlate with the location of the tidal tails. Therefore, objects like those in the galaxy sample are not likely to cause significant disturbances in the stellar sample. The only remaining contaminants are compact galaxies with bluer colors that may not be well represented in the sample of known galaxies. We believe that such objects have mostly been eliminated by our color cut $u^* - g^* \leq 0.4\ mag$. Finally, fluctuations in stellar surface density due to variable interstellar absorption can be ruled out because the mean level of absorption in the region around Pal 5 is low and there is no hint for strong variations (values of E_{B-V} in the maps of Schlegel et al. (1998) range between 0.05 mag and 0.07 mag).

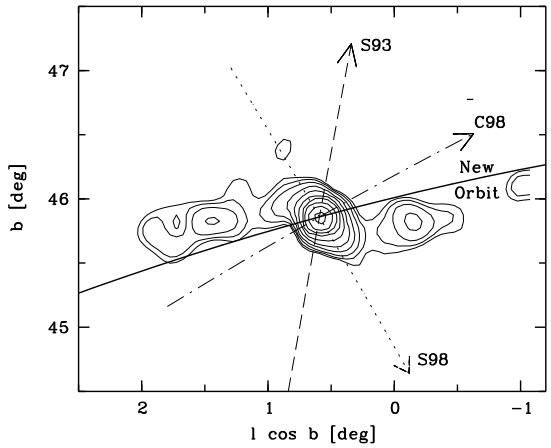

Fig. 3.— Contour plot of the surface density of cluster candidates in galactic coordinates $(l\cos b, b)$ overlayed with different orbital paths of the cluster according to different determinations of its absolute proper motion: S93 = Schweitzer et al. (1993); S98 = Scholz et al. (1998); C98 = Cudworth (unpublished), cited in Scholz et al. (1998). The solid line presents our improved estimate of the orbit based on the geometry and orientation of the tidal tails (fixing the direction of tangential motion) and the proper motions by Cudworth and by Scholz et al. (estimating the tangential velocity).

3.3. Implications for and from the cluster's orbit

The orientation of the tails provides unique information on the direction of the cluster's tangential motion since it is known that the leading and trailing parts must fit in with the inner and outer side of the local orbit, respectively. Fig. 3 reveals that the tails stretch out in the direction of constant b, and that the tangential motion is very likely westward (prograde rotation). The absolute proper motions by Schweitzer et al. (1993) and Scholz et al. (1998) yield very different predictions for the local orbit, although at least the sense of rotation is in agreement. The proper motion given by Cudworth (priv. comm., unpublished revision of the work by Schweitzer et al.) yields a local orbit which lies closer to the tails. From the observed orientation of the tails we estimate that the tangential velocity vector points $\sim 15°$ north of the line of constant b. In order to meet this constraint the proper motion needs to be modified by not more than $0.4\,\mathrm{mas\,yr^{-1}}$ w.r.t. Cudworth's values. We thus adopt $\mu_l \cos b, \mu_b = -0.93, +0.25\,\mathrm{mas\,yr^{-1}}$ for the cluster's proper motion in the galactic rest frame. With these values we obtain an orbit (using the galactic potential of Allen & Santillan 1991) with apo- and perigalactic distances of 19.0 kpc and 7.0 kpc, and with disk passages at -137 Myr, -292 Myr and -472 Myr, taking place at Galactocentric radii of 9.4, 18.4 and, 8.3 kpc, respectively. Similar orbits are obtained with the more detailed galactic potentials of Dehnen & Binney (1998). We tend to believe that the observed overdensities close to the cluster result from the latest disk passage while the clumps in the tails at distances of $\sim 0.8°$ from the cluster might be associated with the earlier passage through the inner disk about 470 Myr ago. This, however, has to be investigated more thoroughly with N-body simulations. The next passage through the galactic disk predicted by our model orbit will be in 113 Myr and will happen close to perigalacticon. If true, this will again produce a strong tidal shock that may eventually dissolve the cluster completely.

3.4. Outlook

The SDSS will eventually cover a much larger region around Pal 5 than currently available. Larger area coverage will enable us to constrain the orbit and mass loss more tightly. We can further constrain our model orbit by obtaining radial velocities of stars in the tails. We predict a local radial velocity gradient of $5.7\,\mathrm{km\,s^{-1}\,deg^{-1}}$, i.e. $\sim 9\,\mathrm{km\,s^{-1}}$ difference between the radial velocities of stars in the two tidal tail clumps. Since Pal 5 contains very few luminous red giants, even fewer are expected in its tails, thus kinematic studies will have to concentrate on fainter stars requiring large telescopes.

The Sloan Digital Sky Survey (SDSS) is a joint project of The University of Chicago, Fermilab, the Institute for Advanced Study, the Japan Participation Group, The Johns Hopkins University, the Max Planck Institute for Astronomy, New Mexico State University, Princeton University, the United States Naval Observatory, and the University of Washington. Apache Point Observatory,

site of the SDSS, is operated by the Astrophysical Research Consortium. Funding for the project has been provided by the Alfred P. Sloan Foundation, the SDSS member institutions, the National Aeronautics and Space Administration, the National Science Foundation, the U.S. Department of Energy, and Monbusho. The SDSS Web site is http://www.sdss.org/.

REFERENCES

Allen, C., & Santillan, A., 1991, RMxA&A, 22, 255

Chernoff D.F., Weinberg M.D., 1990, ApJ, 351, 121

Combes, F., Leon, S., & Meylan, G., 1999, A&A, 352, 149

Dehnen, W., Binney, J., 1998, MNRAS, 294, 429

Djorgovski S., Meylan G., 1994, AJ, 108, 1292

Fukugita, M., Ichikawa, T., Gunn, J.E., Doi, M., Shimasaku, K., & Schneider, D. P., 1996, AJ, 111, 1748

Gnedin, O.Y., Ostriker, J.P., 1997, ApJ, 474, 223

Grillmair, C.J., Freeman, K.C., Irwin, M., & Quinn, P.J., 1995, AJ, 117, 1792

Gunn, J.E., Carr, M., Rockosi C., et al., 1998, AJ, 116, 3040

Harris W.E., 1996, AJ, 112, 1487

Ivezic, Z., Goldston, J., Finlator, K., et al., 2000, AJ, 120, 963

Lehmann, I., & Scholz, R.D., 1997, A&A, 320, 776

Leon, S., Meylan, G., & Combes, F., 2000, A&A, 359, 907

Schlegel D.J., Finkbeiner D.P., & Davis M., 1998, ApJ, 500, 525

Scholz, R.-D., Irwin, M., Odenkirchen, & Meusinger, H., 1998, A&A, 333, 531

Schweitzer, A.E., Cudworth, K., & Majewski, S.R., 1993, in ASP Conf.Ser. 48, The Globular Cluster-Galaxy Connection, ed. G.H. Smith and J.P. Brodie (San Francisco: ASP), 113

Sandage, A., & Hartwick, F.D.A., 1977, AJ, 82, 459

Silverman, B.W., 1986, Density estimation for statistics and data analysis, London, Chapman & Hall

Smith, G.H., 1985, ApJ, 298, 249

Trager, S.C., King I.R., & Djorgovski, S., 1995, AJ, 109, 218

Testa, V., Zaggia, S.R., Andreon, S., Longo, G., Scaramella, R., Djorgovski, S.G., & de Carvalho, R., A&A, 356, 127

Yanny, B., Newberg, H., Kent, S., et al., 2000, ApJ, 540, 825

York, D.G., Adelman, J., Anderson, J.E., et al., 2000, AJ, 120, 1579

This 2-column preprint was prepared with the AAS LaTeX macros v5.0.